

Article

# Indoor Airflow Distribution in Repository Design: Experimental and Numerical Microclimate Analysis of an Archive

Karin Kompatscher <sup>1,\*</sup>, Rick P. Kramer <sup>1,2</sup>, Bart Ankersmit <sup>3</sup> and Henk L. Schellen <sup>1</sup>

<sup>1</sup> Department of the Built Environment, Eindhoven University of Technology, P.O. Box 513, 5600 MB Eindhoven, The Netherlands; rick.kramer@maastrichtuniversity.nl (R.P.K.); H.L.Schellen@tue.nl (H.L.S.)

<sup>2</sup> Department of Health, Medicine and Life Sciences, Maastricht University, P.O. Box 616, 6200 MD Maastricht, The Netherlands

<sup>3</sup> Cultural Heritage Agency of The Netherlands, 3800 BP Amersfoort, The Netherlands; b.ankersmit@cultureelerfgoed.nl

\* Correspondence: k.kompatscher@tue.nl



**Citation:** Kompatscher, K.; Kramer, R.P.; Ankersmit, B.; Schellen, H.L. Indoor Airflow Distribution in Repository Design: Experimental and Numerical Microclimate Analysis of an Archive. *Buildings* **2021**, *11*, 152. <https://doi.org/10.3390/buildings11040152>

Academic Editors: Ravi Srinivasan and Karim Ghazi Wakili

Received: 24 January 2021

Accepted: 29 March 2021

Published: 5 April 2021

**Publisher's Note:** MDPI stays neutral with regard to jurisdictional claims in published maps and institutional affiliations.



**Copyright:** © 2021 by the authors. Licensee MDPI, Basel, Switzerland. This article is an open access article distributed under the terms and conditions of the Creative Commons Attribution (CC BY) license (<https://creativecommons.org/licenses/by/4.0/>).

**Abstract:** The majority of cultural heritage is stored in archives, libraries and museum storage spaces. To reduce degradation risks, many archives adopt the use of archival boxes, among other means, to provide the necessary climate control and comply with strict legislation requirements regarding temperature and relative air humidity. A strict ambient indoor climate is assumed to provide adequate environmental conditions near objects. Guidelines and legislation provide requirements for ambient indoor climate parameters, but often do not consider other factors that influence the near-object environment, such as the use of archival boxes, airflow distribution and archival rack placement. This study aimed to provide more insight into the relation between the ambient indoor conditions in repositories and the hygrothermal conditions surrounding the collection. Comprehensive measurements were performed in a case study archive to collect ambient, local and near-object conditions. Both measurements and computational fluid dynamics (CFD) modeling were used to research temperature/relative humidity gradients and airflow distribution with a changing rack orientation, climate control strategy and supply as well as exhaust set-up in a repository. The following conclusions are presented: (i) supplying air from one air handling unit to multiple repositories on different floors leads to small temperature differences between them. Differences in ambient and local climates are noticed; (ii) archival boxes mute and delay variations in ambient conditions as expected—however, thermal radiation from the building envelope may have a large influence on the climate conditions in a box; (iii) adopting night reduction for energy conservation results in an increased influence of the external climate, with adequate insulation, this effect should be mitigated; and (iv) the specific locations of the supply air and extraction of air resulted in a vertical gradient of temperature and insufficient mixing of air, and adequate ventilation strategies should enhance sufficient air mixing in combination with the insulation of external walls, and gradient forming should be reduced.

**Keywords:** indoor environment; cultural heritage storage; archive; monumental building; hygrothermal measurements; CFD modeling

## 1. Introduction

Archives, libraries and museum storage preserve the majority of cultural heritage: for a typical museum, around 90% of the collection is placed in storage and 10% is on display (<https://www.bbc.com/news/uk-england-london-12214145> accessed on 20 February 2021). The indoor climate conditions in these buildings are important to ensure the longevity of objects and reduce degradation risks such as biological, chemical and mechanical degradation. In addition to many other factors, indoor temperature and relative air humidity play

a vital role in collection conservation. Compared to archival buildings, indoor climates in museum galleries with objects on display are frequently researched. In exhibition galleries, the indoor climate parameters can be disturbed by visitor presence acting as a heat and moisture source [1] and in archives, thermal and hygric inertia of the stored objects could be of influence [2]. The current paradigm on environmental conditions in archives includes the preference for a low temperature ( $T$ ) and a relative humidity ( $RH$ ) that is more or less stable around the midrange [3–5]. A high incorrect  $T$  can accelerate the chemical degradation of organic material (e.g., cracking of leather bindings, yellowing of paper). Fluctuations in  $T$  result in fluctuations in  $RH$  which might, in case of continuous high  $RH$ , accelerate mold growth, and the warping and curling of susceptible paper materials [6–8]. In a recent study, the effect of cleaning procedures in a museum building on the variability of  $RH$  was found. The use of water in the cleaning procedure should be minimized to prevent fluctuations [9].

Guidelines and legislation often provide ideal values for ambient indoor climate parameters to ensure low degradation risks, i.e., strict prescriptive values resulting in a strictly controlled indoor climate. Meeting the requirements often means that archives are needed to implement a heating, ventilation and air-conditioning (HVAC) unit to compensate incorrect indoor  $T$  and  $RH$  conditions caused by, among other factors, the poor quality of the building envelope.

British legislation adjusted its storage requirements in recent decades from strict setpoints for  $T$  and  $RH$  [10] towards more tolerant setpoints [11]. Dutch archival legislation is, compared to the current British legislation, very prescriptive and strict about the permissible indoor climate [12]. In recent years, two types of storages have been distinguished in the Dutch archival legislation: long-term, i.e., for over twenty years, and short-term, i.e., up to twenty years. The specifications for  $T$  and  $RH$  are less strict for short-term storage spaces. Instead of an 18 °C setpoint with an allowed fluctuation of ±2 °C for long-term preservation, a bandwidth is allowed for short-term preservation as long as the temperature stays within the range of 16–20 °C and the permissible fluctuations for  $RH$  have been doubled from ±5% to ±10%. Long-term specifications require more energy to maintain than the short-term specifications, even though the minimum and maximum values for  $T$  are similar.

Archives and libraries house a bulk of hygroscopic materials (i.e., large paper collections). The limited occupancy of staff and visitors results in less need for ventilation and thermal comfort. This has resulted in a new way of thinking about ventilation purposes in archives and opened opportunities for possible energy savings. Several studies investigated possibilities such as intermittent conditioning [13,14], increasing building envelope quality [15] and seasonal setpoint adjustment [6,16].

In addition to the adjustment of the climate control in archives, multiple building physics-related measures have been investigated in the literature. Limiting external factors such as the external climate is required for a storage environment. Passive measures are pursued such as reducing air infiltration by sealing cracks and increasing the thermal insulation of walls. Optimizing ways to limit the impact of the outdoor climate has resulted in a plethora of studies on passive and low-energy museum storage and archive buildings [17–23]. The underlying thought is that the storage facility needs a large hygrothermal storage capacity and an airtight building envelope to reach a stable  $T$  and  $RH$  for preservation purposes. Thermal buffering is also a result of the ground and building envelopes' thermal capacity. External seasonal fluctuations are delayed and mitigated through buffering. In addition to a stable (and low)  $T$ ,  $RH$  buffering is mainly caused by the collection materials and the building's walls. Small HVAC systems with limited capacity may be needed to provide (de)humidification and pollutant filtering. The limited energy demand may be provided by renewable energy sources such as solar panels. Holl et al. [24] suggested that a newly built depot building should consider passive measures to reduce energy demand—ideally, with the so-called archival concrete which has high water retention properties and low initial moisture levels. Another study advocates

passive measures whilst noting that infiltration needs to be kept low. This would maintain a low level of daily fluctuations and may reduce investments in air-conditioning systems [25]. Smedemark et al. compared spatial distributions for  $T/RH$  between a semi-passive repository without mechanical ventilation compared to a repository with an HVAC system [23]. The study showed, with data collected from an extensive grid measurement, that both repositories upheld an acceptable climate performance. The study was performed in a purpose-built building for safekeeping heritage. The investigated repositories have no external walls but are connected to service areas [23].

The deterioration mechanisms of unstable objects highly depend on environmental conditions [26]. In order to increase the longevity of archival collections, enclosures such as archival boxes or envelopes have been largely adopted in this field. These enclosures form an extra layer that mitigates disruptive ambient climate variations. Studies based on laboratory experiments exist and a number of in situ measurements in operational archives have been performed. Wilson et al. [27] showed the effect of objects in enclosures in open shelves based on risk mitigation and dust transfer. Limited research has been found on in situ hygrothermal measurements in archival boxes. The National Archives in the UK showed that relative humidity in an archival enclosure, such as an archival box or envelope, can have different values compared to the ambient conditions in the used environmental test chamber [28]. Clare et al. described that under certain circumstances, the  $RH$  in a box increases beyond the ambient  $RH$  conditions. Such a circumstance is, for example, a quick drop in ambient  $RH$  conditions. Humidity is being delayed in the archival box even if the levels are higher than ambient conditions. The microclimate shows fluctuations even when it has not reached the ambient level. This study showed that it would take approximately over a week to reach an equilibrium inside the box when ambient conditions have changed significantly [28]. In a white paper, the Image Permanence Institute disclosed several conclusions drawn from a large study where photographs, paper, books and the use of different enclosures were tested in laboratory settings [29]. Intentional temperature set-backs, based on energy saving potential, showed that the temperature change was distributed quite fast through the used samples. Only hours passed for the core of the test sample to reach thermal equilibrium. Moisture variations seemed to be mitigated due to the used enclosures. The test samples showed a distinct difference between the surface and the core. One of the major conclusions was that the  $RH$  fluctuations in the test samples in the box were less dependent on change in ambient  $RH$ , but more on temperature change.

Given the current trends in designing and developing low-energy storage facilities and the more traditional required climate specifications in Dutch Archives, the question is to what extent the dependence on technology (i.e., HVAC) can be reduced while still maintaining appropriate conditions for collection preservation. Smedemark et al. [23] showed that semi-passive climate control is promising, however, the conclusions are valid for repositories in purpose-built storage facilities with limited external walls. External temperatures of below 0 °C during wintertime and above 25 °C during summer were present. Indoor conditions of archival or library facilities housed in existing or even historic buildings are more likely to be affected by conditions in adjacent rooms or external climate conditions [14]. Storage spaces are often packed with archival collections in special archival racks. The large amounts of hygroscopic material is able to stabilize  $RH$  when ventilation flows are reduced [2,30]. The archival racks form bluff bodies meaning they separate airflow and stagnant air zones might occur resulting in microclimates. Stable and homogeneous conditions are largely dependent on the airflow distribution in a room. In repositories, an air handling unit (AHU) is to a large extent responsible for the distribution and good mixing of air. It is therefore important to understand to what extent airflow is influenced by the repository design. Guidelines and legislation provide requirements for ambient indoor climate parameters, however, they do often not consider other factors that influence the near-object environment such as the use of archival boxes, airflow distribution and archival rack placement.

This study aimed to provide more insight into the relation between the ambient indoor conditions in repositories and the hygrothermal conditions surrounding the collection. Through an experimental campaign, hygrothermal indoor conditions provided insight into the use of archival boxes to create a favorable preservation microclimate. A numerical study was conducted to help investigate whether the HVAC air supply and extraction and the archival rack placement had an influence on the indoor airflow distribution. Without increasing the risk to the archival collection, computational modeling provided quantitative means to investigate the results from the measurements and whether reducing the air supply during a limited amount of time had influence on stable indoor conditions suitable for the preservation of heritage collection.

The following research questions have been formulated to structure the current study:

- How do the ambient hygrothermal conditions of the repository affect archival box hygrothermal conditions?
- In what way does the orientation of archival racks influence the air distribution of the supplied air and therefore the homogeneity of ambient air conditions?
- what is the effect of a reduction in ventilation at night on the hygrothermal conditions and air distribution throughout the repository?

This paper is structured as follows: in the next section, the used methodology of the experimental and numerical research is described in detail. Results are discussed in the section thereafter and lastly, the discussion section will end with the conclusions drawn.

## 2. Materials and Methods

### 2.1. Case Study Description

The case study investigated in this research was an archival institution situated in Leiden, the Netherlands. The collection present in the repositories comprises archival collection (i.e., books, newspapers, building plans etc.) and archaeological collection of Leiden and surroundings. The majority of the archival collection is housed in storage racks and is placed in some type of enclosure such as archival boxes and envelopes to protect it from external risks (Figure 1, a building plan can be found in Figure A1).



**Figure 1.** External impression (image from [www.visitleiden.nl](http://www.visitleiden.nl), accessed on 20 February 2021).

Several functions are housed in the building: (i) publicly accessible areas such as an auditorium and research facilities; and (ii) internal areas such as the repositories and offices. These areas are divided over multiple, interconnected buildings. Part of the building is an enlisted building. Most repositories with a ground surface of  $836\text{ m}^2$  are located in a five-story high tower (see Figure A1 in Appendix A). The other part of the archival collection ( $652\text{ m}^2$ ) can be found in a two-story building connected to the general, public rooms such as a reading room and auditorium. This study focused on the repository tower. Per floor, the repository takes up approximately  $170\text{ m}^2$  and with a height of 2.3 m, the repository volume is  $391\text{ m}^3$  (Figure 2 shows one repository floor of the tower). This

part of the building is an extension with a brick cavity wall with low thermal resistance ( $U$ -value > 2 W/m<sup>2</sup>K). On all floors, small repetitive windows are present on both the east and west sides of the building. The windows are internally blinded by a layer of dark paint to prevent internal solar irradiation.

The climate control system of the repository is an older heating, ventilation and air-conditioning (HVAC) system (>25 years old) which is able to control both the temperature and relative humidity in the repositories, by means of heating, cooling, humidification and dehumidification. It also has an F9 filter to collect fine dust and particles (1–10 µm). The AHU makes use of recirculation (90%) and fresh air (10%) mixing. The AHU supplies conditioned air to all floors. Combined  $T/RH$  sensors in the return ducts of each floor are averaged and determine the control action. Figure 2 shows the floor plan of repository number 6 (located on the fourth level of the tower), moreover, a schematic representation is given for the supply ducts (orange) and extraction ducts (blue). Figure 3 shows the section of the repository tower including depots 3–7. Over the entire width of the room, ducts were placed at the top of the walls. Inlet grids (75 mm × 225 mm) were placed every other meter to provide an even inlet profile. Climate control adopted a temperature setpoint of 16.5 °C with a permissible fluctuation of ±1 °C. During summer, the inlet conditions could be even lower to reach the adopted room setpoint. Due to the low inlet  $T$  conditions, it is difficult to dehumidify the supply air. This resulted in an adopted  $RH$  specification of 55% with a permissible fluctuation of ±5%  $RH$  by the institution. Visitors are incidentally allowed in the repositories for special tours. The conservation specialist retrieves items for a special restoration area to work on the preservation of the objects. Visits to the repositories are limited.

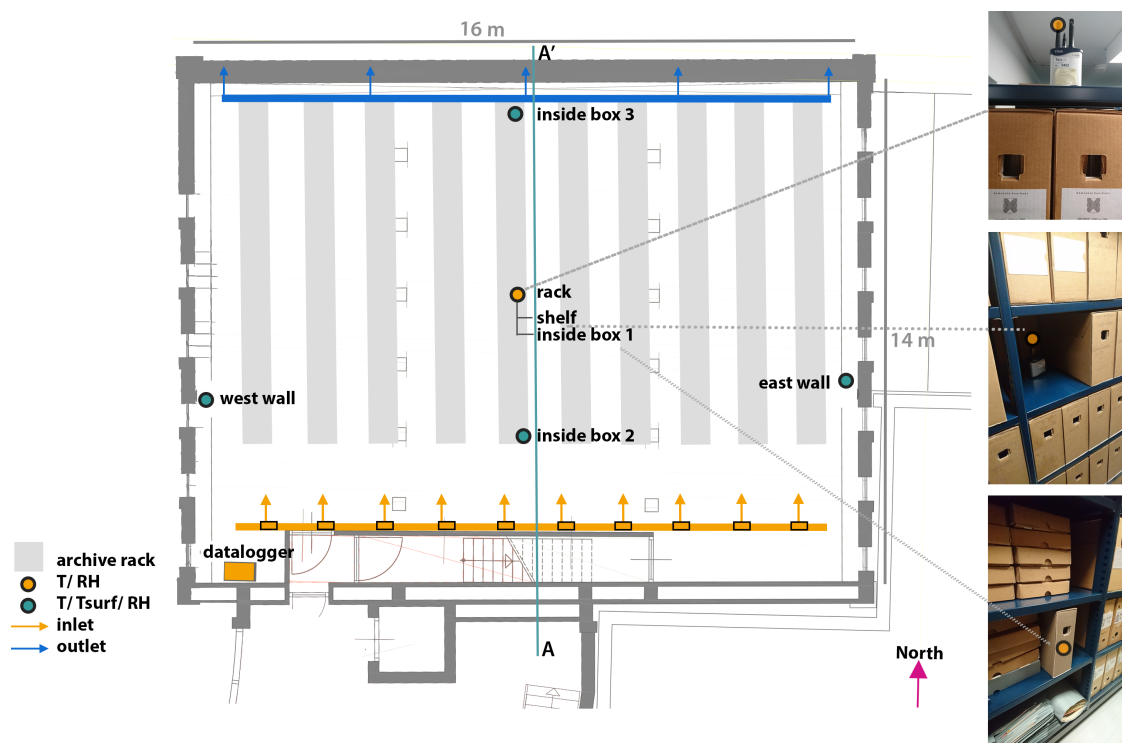


**Figure 2.** Floor plan of depot 6 with the locations of the experimental measurement campaign.

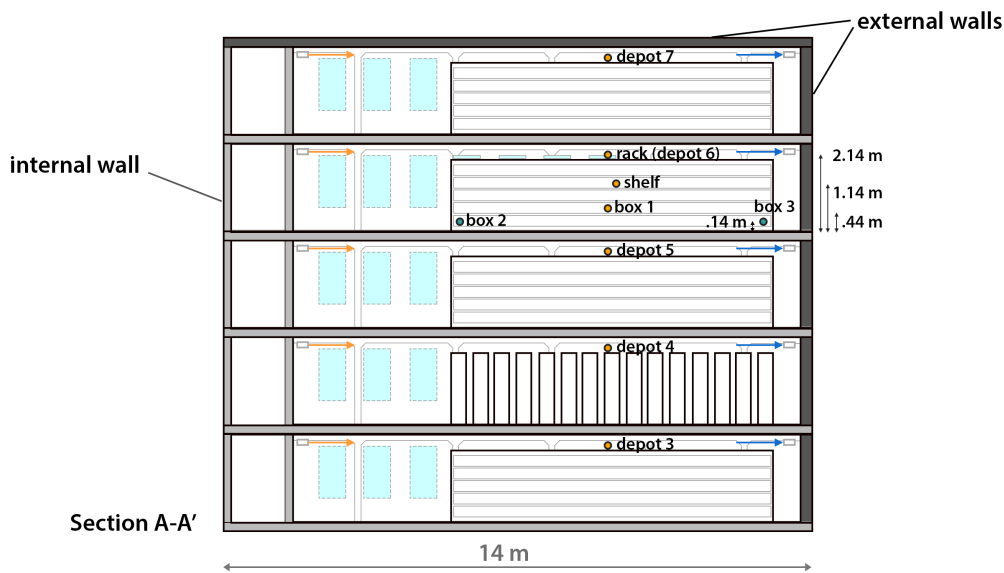


**Figure 3.** Vertical section A–A' shows a schematic of the repository tower (floors 3–7) with the locations of the  $T/RH$  sensors.

## 2.2. Environmental Monitoring

To gain insight into the indoor climate conditions of a specific archive and the effect of archival boxes,  $T$  and  $RH$  measurements were performed using combined  $T/RH$  Eltek sensors [31] with a time interval of 10 min and a measurement accuracy of  $\pm 0.4\text{ }^{\circ}\text{C}$  and  $\pm 3\%$   $RH$ . An Eltek RX250AL data logger was used to collect, store and send data to a server at the Eindhoven University of Technology. This campaign started in September 2017 and lasted until June 2019. The measurement positions were determined by using a climate scan that determined the deviating local indoor microclimates.

### 2.2.1. External Climate Conditions

External climate conditions were retrieved from the Royal Netherlands Meteorological Institute. These data were collected from a location approximately 5.5 km from the repository location in the city of Leiden. External climate conditions were measured on an hourly basis. Table 1 shows the seasonal statistical parameters for the year 2018.

**Table 1.** Overview of the external climate conditions using statistical parameters.

	$T_{average}$ ( $^{\circ}\text{C}$ )	$T_{std}$ ( $^{\circ}\text{C}$ )	$T_{max}$ ( $^{\circ}\text{C}$ )	$T_{min}$ ( $^{\circ}\text{C}$ )	$RH_{average}$ (%)	$RH_{std}$ (%)	$RH_{max}$ (%)	$RH_{min}$ (%)
Winter	3.9	3.9	14.3	-8.3	81	13	100	35
Spring	14.7	4.8	28.8	1.2	79	16	100	24
Summer	17.3	4.7	34.6	2.5	78	16	100	24
Autumn	8.4	4.7	25.1	-3.1	86	10	100	48

### 2.2.2. Measurement Locations

The area of interest comprised five floors of archival storage space in the *repository tower* of the building. Per repository floor, the ambient hygrothermal conditions were measured with a combined  $T/RH$  sensor placed in the center of the room (the sensor location is called *rack shelf* in Figure 2). On the fourth level of the repository tower (room name: *depot 6*), extra sensors were added to gain insight into the possible vertical and horizontal stratification of the indoor climate conditions. The vertical measurement positions are (i) on top of an archival rack; (ii) in the center of the rack on a shelf; and (iii) on the bottom part of the rack in an archival box (Figure 2, photographs on the right). The repository tower has

three external walls (east, north and west) and one internal wall (south) which is adjacent to a hallway connecting the tower to the listed building. In depot 6, two sensors were placed near the east and the west walls and a connected surface temperature sensor was placed on the surface of the walls. At the beginning of the year 2019, two extra sensors were placed inside boxes 2 and 3. This was done to investigate the influence of microclimates on the climate conditions in the archival box.

### 2.2.3. Data Processing and Analysis

The measurements were used to gain insight into the present indoor climate behavior of the repositories. Ambient climate conditions in the different repositories were compared with the cumulative distribution function (CDF) per floor level for the entire measurement period. The slope of the curve gives information on the stability of the climate. The steeper the curve (slope is large), the more constant the variable is (in this case either  $T$  or  $RH$  is plotted). If the curve is relatively flat (slope is small), there is a large spread in measured values. The weekly, daily and hourly short-term fluctuations were plotted for both parameters. Biological risk based on high temperatures and/or high relative humidities are depicted through the fungal growth curve [32]. Biological deterioration could severely damage archival collection objects [7]. Chemical risk is presented by the lifetime multiplier (LM) (Equation (1)):

$$LM_x = \left( \frac{50\%}{RH_x} \right)^{1.3^e \frac{E_a}{R} \left( \frac{1}{T_x} - \frac{1}{293} \right)} \quad (1)$$

where  $RH_x$  (%) is the measured relative humidity at time point  $x$ ,  $E_a$  is the activation energy in (J/mol) dependent on the type of material of the object,  $R$  is the gas constant 8.314 (J/mol),  $T_x$  (K) is the temperature in point  $x$ , and  $x$  is a data point in the data series.

The lifetime multiplier is dependent on a reference  $T$  and  $RH$  of 20 °C and 50%, respectively [33]. The percentage of time that the measurement data are within a certain criteria range (in this case, Dutch legislation for long-term preservation) was used to provide information on the preservation conditions for different measurement locations. Object environment measurements were used to assess the preservation conditions in an archival box.

### 2.3. Numerical Study

The finite element modeling software COMSOL Multiphysics version 5.2a [34] was used to investigate the hygrothermal distribution in the repositories and explain the measurement results. With a simplified model, representing the geometry of the fourth floor of the case study, both air velocity and temperature profiles were calculated. Inlet conditions supplied by the current climate system were used as inlet boundary conditions to account for the heat generation due to the ventilation system. The simplification of the model was mainly due to simplification of the geometry to reduce computational complexity (i.e., computational time). The simulations serve as qualitative means to explain the obtained results from the  $T$  and  $RH$  measurements. The case study repository was set-up in such a way that the AHU inlet ducts were situated along the south wall. Several inlet grids supplied air at a height just above the archive racks. Air was extracted from the other side of the room at the north wall (see Figure 4).

The numerical model consisted of a heat transfer with a surface-to-surface radiation model to account for radiation influences. The model combined convective heat transfer and radiant heat transfer. Assuming a well-mixed air zonal model is insufficient, and therefore, computational fluid dynamics (CFD) was included to predict temperature distributions in the indoor air and heat transfer near the walls [35]. The heat transfer and fluid flow (CFD) modules of COMSOL were coupled through a multiphysics node. For this study, the k- $\epsilon$  turbulence model was used to provide insight for this general-purpose case. Internal gains through light fixtures and employees or visitors entering the repository were considered neglectable. Employees might enter the repository for a short period of time

(<10 min) to retrieve an object and take this to another room for investigation. This was not done on a regular basis. Light is automated to switch on and off based on movement.

Figure 4A shows the model geometry setup for the numerical study. The repository, where fixed storage racks were placed in parallel to the inlet ducts supply direction (red arrows), is shown in Figure 4A. The red inlet grid has a height of 75 mm. On the other side of the room, a similar opening was assigned as outlet (dark blue). Measurement values of the external temperature—gained from the experimental campaign—were placed as boundary conditions on the external wall. The floor, ceiling and internal wall had boundary conditions based on the measurements from these surfaces. A 3D-section of one meter width was used to research the distribution of supplied air around the storage racks in the 3D model (Figure 4A, orange segment). The 2D plane of analysis was marked as a blue plane in Figure 4B,C. The *symmetry* boundary condition was used to reduce the computational time and included all necessary elements surrounding the investigated 3D section. Figure 4C shows the model with racks perpendicular to the air supply direction.

Hygrothermal distribution was investigated by means of different scenarios where the rack configuration, extract position and collection filling ratio were varied. Changes in the model were based on geometry differences (rack orientation, extract position and collection filling ratio) and by altering the inlet boundary conditions (night reduction). Table 2 provides an overview of the investigated scenarios.

Table 3 provides an overview of the boundary conditions of the numerical model. The four geometry scenarios, as described in Table 2, were used for multiple simulations. The time step interval was set to 30 min for all simulations to maintain good convergence.

**Table 2.** Overview and description of the different scenarios.

Scenario	Geometry	Description
A	Parallel racks	This configuration is commonly found in the repository. The archival racks are considered bluff bodies and represent collection filling up the racks (filling rate = 100%).
B	Perpendicular racks	This configuration is also commonly found in the repository. The archival racks are considered bluff bodies and represent collection filling up the racks (filling rate = 100%).
C	Perpendicular open shelves	This configuration has open shelves to investigate airflow through the different racks and shelves.
D	Night reduction	This configuration represents a change in climate control. The Air Handling Unit can be turned off during closing hours (18:00 h–06:00 h) by reducing the inlet conditions to no ventilation. During these hours, no employees are present in the repositories and no disruptions are expected. The building envelope of the archive has low thermal insulating properties. The external climate boundary conditions are based on a climate file from the Royal Netherlands Meteorological Institute (KNMI). Using night reduction as a control strategy would benefit energy savings [14].
E1	Parallel racks low extract	This configuration investigates whether placing the outlet near the floor would increase the mixing of air and as a result, promote more stable indoor climate conditions.
E2	Perpendicular racks low extract	This configuration investigates whether placing the outlet near the floor would increase mixing of air and as a result, promote more stable indoor climate conditions.

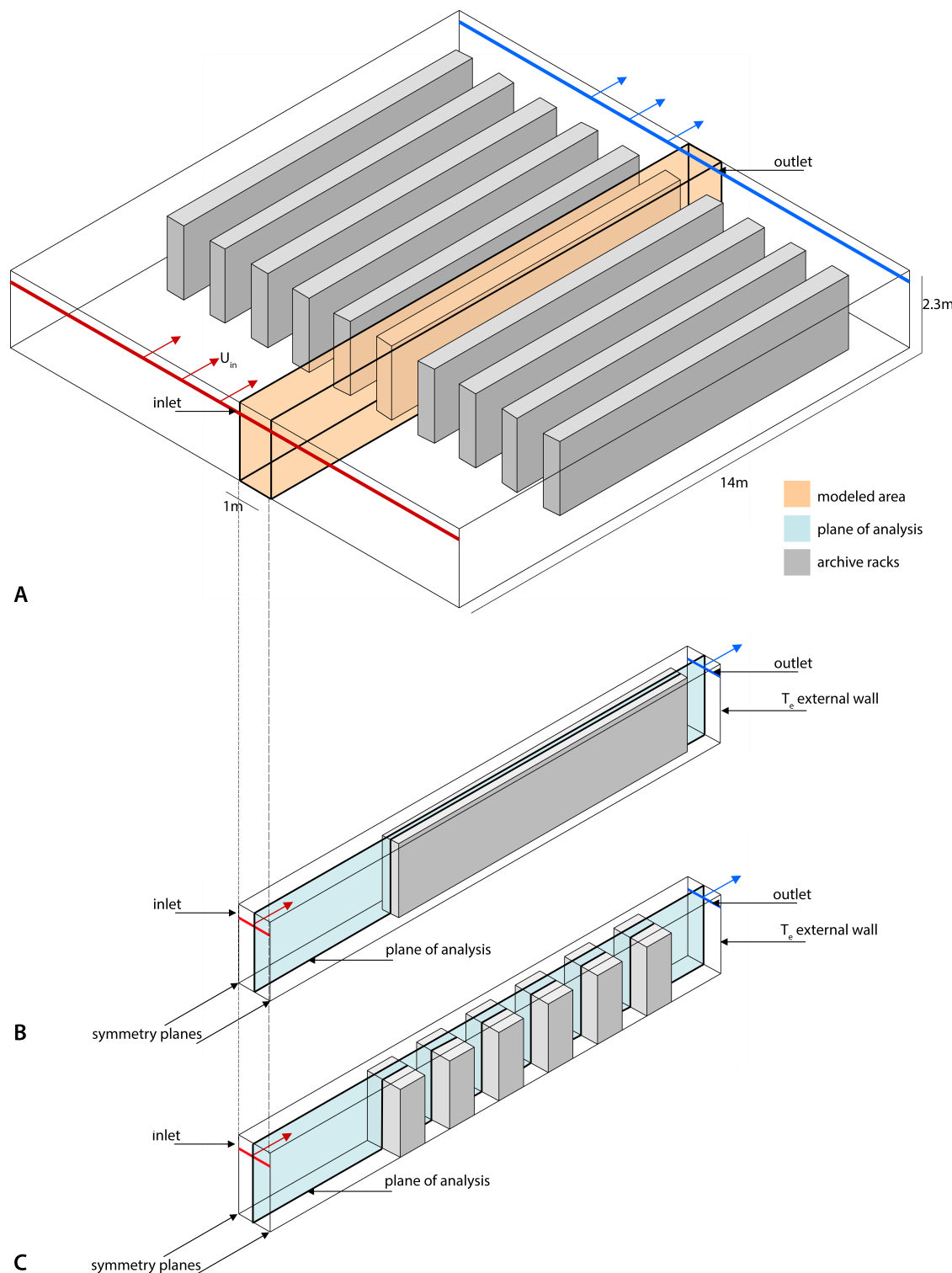


**Figure 4.** Schematic geometry and boundary conditions for the 3D model for the archival racks parallel to the inlet direction scenario (**A,B**) and 3D representation of the perpendicular scenario (**C**) with open shelves.

**Table 3.** Boundary conditions and settings of the numerical model.

Physics modules	Conjugate heat transfer with surface-to-surface radiation; non-isothermal flow
Radiation settings	Wavelength dependence of emissivity: constant
Surface emissivity factor	0.9 (colored paint—estimated value)
Inlet	$U_{in} = 1 \text{ m/s}$ , $T_{in}$ = interpolation from on-site measurements
Outlet	$P = 0 \text{ Pa}$
$T_e$	KNMI measurements
Internal walls	Heat flux based on on-site measurements from adjacent rooms
Turbulence model type	reynolds averaged navier-stokes (RANS)
Turbulence model	k- $\epsilon$
Reynolds number at inlet	1166
Include gravity	yes

Multiple statistical operators were used to quantify whether the model is considered to be accurate. Measurement data and simulated outcome were compared with the fractional bias (FB), fraction of data (FAC), normalized mean bias error (NMBE) and coefficient of variation of the root mean square error (CV RMSE). The latter two are more commonly used in building simulation [36–38]. The FB and FAC1.05 are commonly used for CFD studies and are leading in the current CFD study [39]:

$$FB = \frac{\bar{O} - \bar{P}}{0.5 \cdot (\bar{O} + \bar{P})} \quad (2)$$

where  $O$  are the observed (measured) data points and  $P$  are the predicted (simulated) data points:

$$FAC1.05 = \frac{1}{N} \sum_{i=1}^N n_i \quad (3)$$

where:

$$n_i = \begin{cases} 1 & \text{for } 0.95 \leq \frac{P_i}{O_i} \leq 1.05 \\ 0 & \text{else} \end{cases}$$

The factor 1.05 is commonly used for temperature comparisons. Where  $N$  is the number of data points,  $P_i$  are the predicted values and  $O_i$  are the observed values:

$$MBE (\%) = \frac{\sum_{i=1}^N (O_i - P_i)}{O_i} \quad (4)$$

$$CV \text{ RMSE} (\%) = \frac{\sqrt{\sum_{i=1}^N (O_i - P_i)^2 / N_p}}{\bar{O}_i} \quad (5)$$

### 3. Results

This section describes the results gained from the measurement campaign. The section starts with results from the ambient indoor climate conditions in the repository tower. The next section explains the results found in depot 6 where more sensors were placed and different local microclimates were investigated during the summer and winter seasons.

#### 3.1. Ambient Indoor Climate Conditions

Figure 5 (top) shows the cumulative distribution function (CDF) per floor level for the entire measurement period. The majority of measured values were similar and this is reflected in the steep slopes for depots 3, 4 and 7. In general, the average temperature values were between 16 °C and 18 °C and the average relative humidity was between 55% and 60%. Multiple statistical operators were calculated and are presented in the Appendix A. The subfigures showed the CDF plots for the weekly, daily and hourly fluctuations in the temperature and relative humidity. These were calculated by taking the difference

between the minimum and maximum values within the specified time. Temperature changes were small and limited to 2 °C for daily and weekly fluctuations. No obvious differences between the floors stood out for temperature changes. This showed that the temperature values could be considered rather constant.

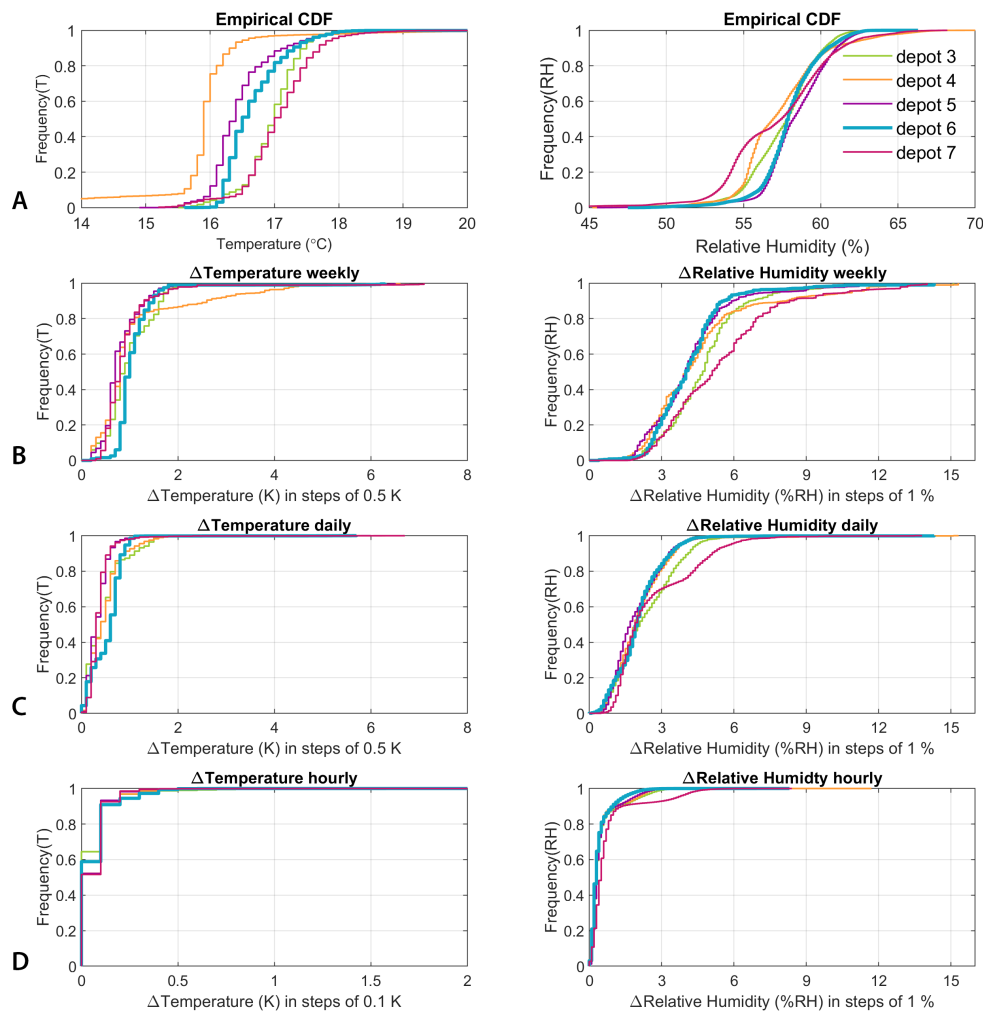


**Figure 5.** Cumulative distribution function (CDF) plots for all floors (A) during the year 2018. Going from top to bottom are the average short fluctuations for the weekly, (B), daily (C) and hourly (D) values presented in the graphs for temperature (left) and relative humidity (right). The legend in the top right subgraph is representative for all subgraphs.

The largest fluctuations in the relative humidity were found in repository 7. Both the daily and weekly relative humidity fluctuations showed a large spread for all floors. This means that the relative humidity fluctuations that occurred throughout the year were not as stable as the measured temperature values. The majority of hourly RH changes was below 3%/h (Figure 5, D-right graph).

For all depots, an assessment was performed to see the percentage of time and whether the  $T/RH$  requirements for Dutch archival legislation *long-term conservation* were met. The measurement locations evaluated in Table 4 represent the average conditions of the different depots and were placed in the center of each depot. As soon as either  $T$  or  $RH$  was not met, the criteria were marked as not OK.

The Lifetime Multiplier (LM) was used to assess possible chemical degradation for paper objects. Table 4 provides the results of these calculations. Though the Dutch archival legislation criteria in most depots were not met, the Lifetime Multiplier showed values

over 1.0, meaning that the objects would last over one lifetime. This can be ascribed to the low temperatures present in the depot areas and the reference conditions the LM equation's use of  $20^{\circ}\text{C}/50\%$  (see Equation (1)).

**Table 4.** Assessment parameters for the different repository levels. The assessment criteria were based on the Dutch Archival Legislation [12]. The Lifetime Multiplier is calculated for paper material.

	Criteria OK— $18 \pm 2^{\circ}\text{C}$ and $50 \pm 5\%$ (%)	LM (-)
Depot 3	13	1.27
Depot 4	10	1.5
Depot 5	5	1.32
Depot 6	7	1.31
Depot 7	31	1.28

### 3.2. Local Microclimate (Archival Box)

To evaluate the local indoor microclimates found in repository 6, Figure 6 shows the yearly results of the different sensors placed in repository 6. Figure 6A shows the measured data of  $T/RH$  in color and the dashed lines are the predicted spore germination time (starting from 75% RH as a limit for biologically recyclable materials) [40]. This quickly showed the possibility of increased risk for biological degradation.

Figure 6 also showed the allowed fluctuation according to the Dutch archive legislation represented by the dark gray square. The amount of dots plotted in this square was the amount of measurements complying with the legislation requirements. As can be seen, the number of measurement points within this square was very little. Overall, the temperature was somewhat lower than the required specifications as defined by the archival legislation. The lower temperature did not result in an increased risk to the archival collection and even increased the Lifetime Multiplier (archival box 1 LM = 1.35 while the legislation criteria were met 0% of the time). The relative humidity was rather high. High relative humidity near the external wall shows an increased risk of mold growth when it exceeds the limit. During the measurement period, the climate conditions did not increase the overall risk of biological degradation.

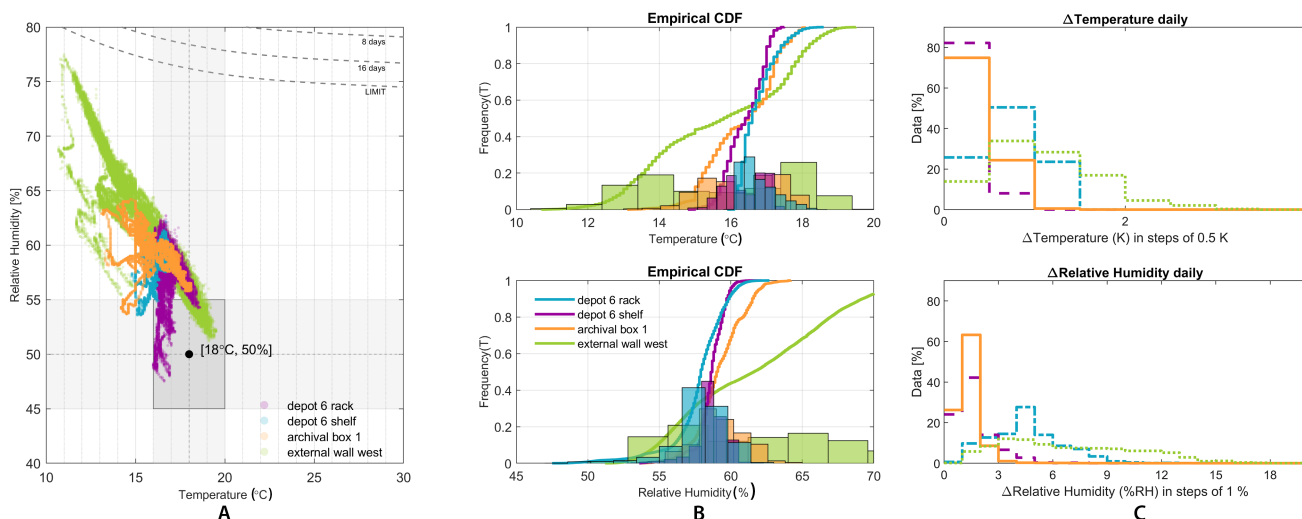


**Figure 6.** Data collected over a year compared to the Dutch archival legislation (A), empirical cumulative distribution function for  $T$  (B, upper) and  $RH$  (B, lower). The remaining graphs show the average short daily fluctuations for temperature (C, upper) and relative humidity (C, lower).

The cumulative distribution function shows that the spread in  $T$  and  $RH$  over a year of measurements in the archival box (orange) was 14–18 °C and about 10%  $RH$ . Short-term daily fluctuation of  $T$  and  $RH$  were small inside the box. Again, near the external wall, large daily fluctuations for  $T/RH$  were found. Objects placed near these walls might experience increased degradation risks from these short-term fluctuations, such as mold risk.

### Seasonal Influences

Repository 6 was investigated in depth by adding extra  $T/RH$  sensors. Figure 7A,B provide the results of  $T$ ,  $RH$  and Humidity Ratio (HR) measurements in a typical summer and winter week. The sensor placed on top of the archive rack (blue line) showed larger fluctuations in  $T$  and  $RH$  compared to the other two locations. The shelf sensor (magenta line) showed a muted and more stable indoor climate. As expected, the archival box showed muting and delay in both  $T$  and  $RH$ .

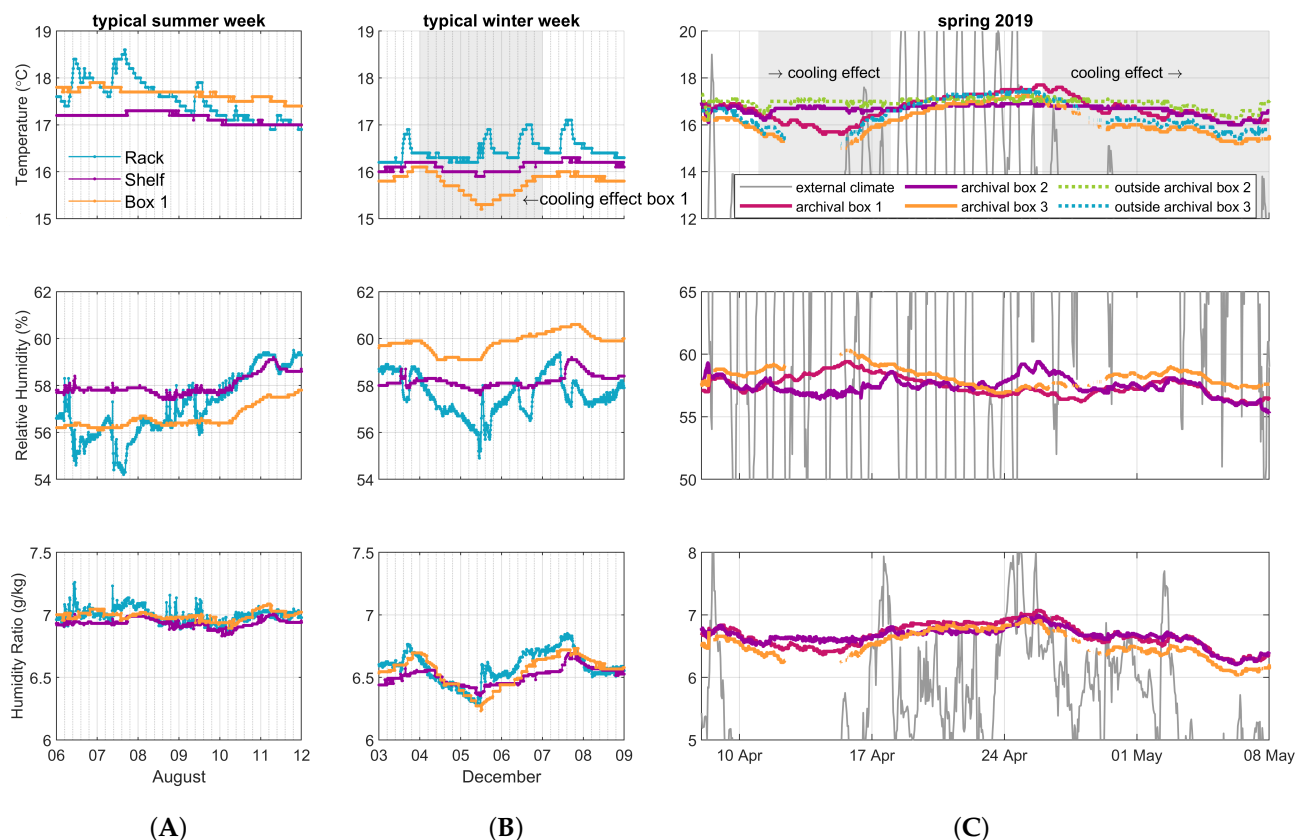


**Figure 7.**  $T$  (up),  $RH$  (center) and  $HR$  (down) results for two typical seasonal weeks in 2018 (A,B). The typical summer and winter weeks show the results of three measurement locations—rack (cyan), shelf (purple) and archival box (yellow).  $T$ ,  $RH$  and  $HR$  for the sensors in archival boxes (continuous line) and  $T$  measurements are just outside the archival boxes (dashed line) for April/May 2019 (C).

The typical winter week showed the temperature declining inside the archival box of about 1 °C. A cooling effect was noticed (3–5 December). While  $RH$  remained relatively stable, the humidity ratio also showed decreasing dips similar to the temperature curve. After noticing this cooling effect happening twice during colder external periods in April and May of 2019 (Figure 7C), additional sensors were placed in three archival boxes. One at the external north wall (box 3) and one near the internal south wall (box 2), (see Figure 2 for exact sensor positions). Extra temperature sensors were also positioned just outside the archival box. The results of the sensors showed that box 3, near the external wall,

experienced low temperatures, while box 2, near the internal wall, showed no decrease in temperature during the period of 10–17 April (Figure 7B). The temperature sensors just outside the archival boxes showed similar trends as the sensors inside the archival boxes. The results showed that the climate inside the archival boxes was influenced by the local temperature, which was a result of the thermal quality of the external wall.

A vertical stratification with a high  $RH$  near the floor and low  $RH$  near the ceiling and vice versa for temperature was noted (Figure 8A). The differences between the preservation microclimate inside the archive boxes are shown in Figure 8B. Differences in microclimate can reach 2 °C and 4%RH with low external air temperatures. As the external air temperature will be much lower in winter and higher in summer, it was expected that these differences become larger. When external air temperature reached values of about 10 °C, the airflow circulation was not sufficient to eliminate the cooling effect near the external north wall. Thermal transmittance through the external wall in combination with the surface radiation resulted in a local microclimate near the external wall with influence on the preservation conditions inside archival box 3. A difference in  $T$  of approximately 2 °C was noticeable compared with the ambient temperature condition in depot 6. A decrease in the thermal transmittance (lower U-value) of the external wall would be required to mitigate this effect.

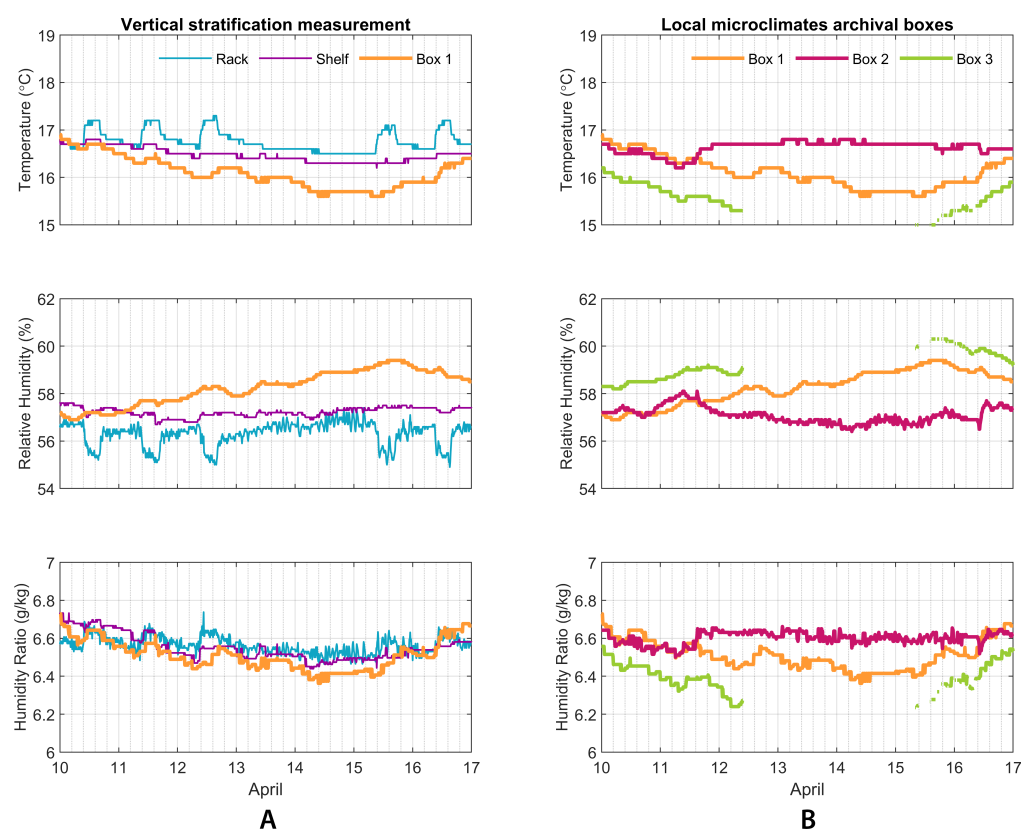


**Figure 8.** Results for the vertical stratification measurements (A) and local microclimate conditions (B) found in archival boxes during the period 10–17 April.

#### 4. Numerical Results

This section shows the results of the validation of the computational model by comparing the data gained from the experimental campaign in repository 6, with the data gained from the numerical study of reference scenario A, the archival racks parallel to the air supply direction. The results from modeling scenarios A–D are given in later paragraphs.

#### 4.1. Calibration

A period of 7 days (10–16 April 2019) was modeled during the numerical study. This timeframe represented a critical period for the indoor climate preservation conditions due to low external temperature conditions (see Figures 7C and 8) and as a result, a dip in  $T$  was observed in the archival box. The external temperature was below 0 °C during this period. These external conditions were used in all scenarios to verify whether the dip in  $T$  through thermal radiation could be reproduced for different scenarios.

After performing a sensitivity analysis on the mesh size, the computational mesh consisted of a physics-controlled mesh with a COMSOL pre-calculated “normal” element size (Figure 9), the number of elements in the plane of analysis was 4560 for scenario A; 9280 for scenario B; 26,608 for scenario C; and 158,278 elements for the entire model (Figure 4—orange segment).

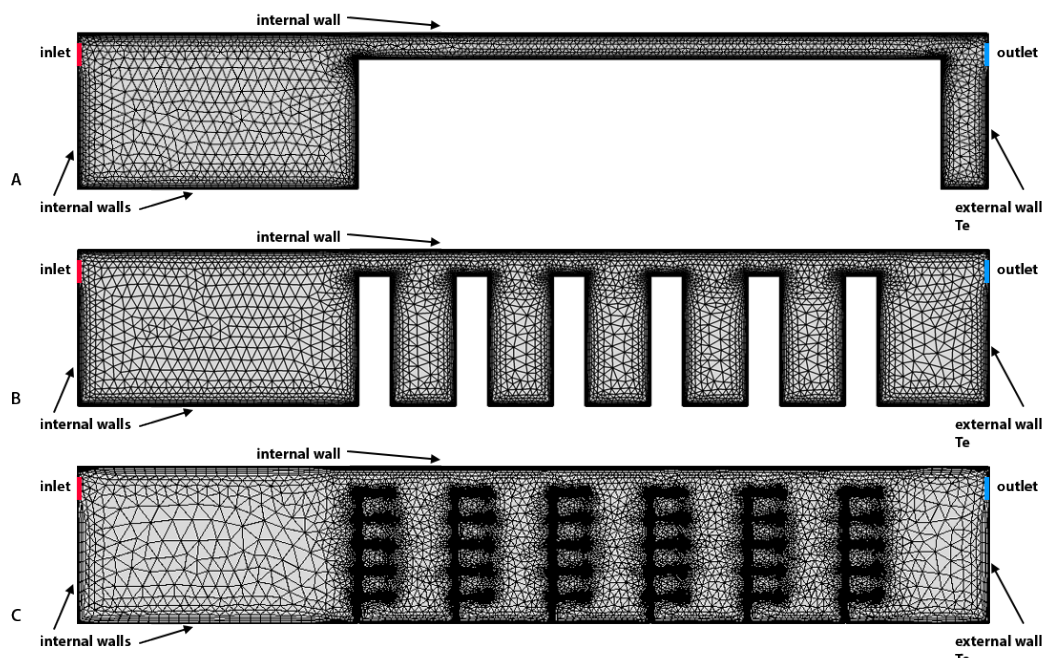


**Figure 9.** Computational mesh in the plane of analysis for the geometry with parallel racks (A); perpendicular racks (B); and the geometry of perpendicular racks with open shelves (C).

Figure 10A shows the evaluation grid set up to compare the numerical outcome with the measurement locations of the experimental campaign. The grid provided evaluation positions every 1 m for a horizontal stratification evaluation and every 40 cm for a vertical stratification evaluation, both coinciding with te measurement locations.

Figure 10B shows the comparison between the measurement positions and the calculated evaluation locations. Good agreement between the measurements and calculated values was reached between  $T_i$ rack and location 9f (Figure 10C), as is shown in the statistical parameters of Table 5. The comparison between the  $T_i$  shelf and its location in 9d shows good agreement according to the statistical operators in Table 5; however, Figure 10 shows that the measurements show more muting of the  $T$  and RH fluctuations between the shelved.  $T_i$  shelf was placed in an occupied rack (see Figure 2) whereas the numerical model does not take buffering from the collection into account.

Table 5 provides the full overview of the comparison between the numerical model and the measurement data. The model was evaluated in locations 9b, 9d and 9f. The RMSE for location 9b, which is compared with measurement data inside archival box 1, is not in agreement (red), which can be clarified by the box not being modeled as a separate entity.

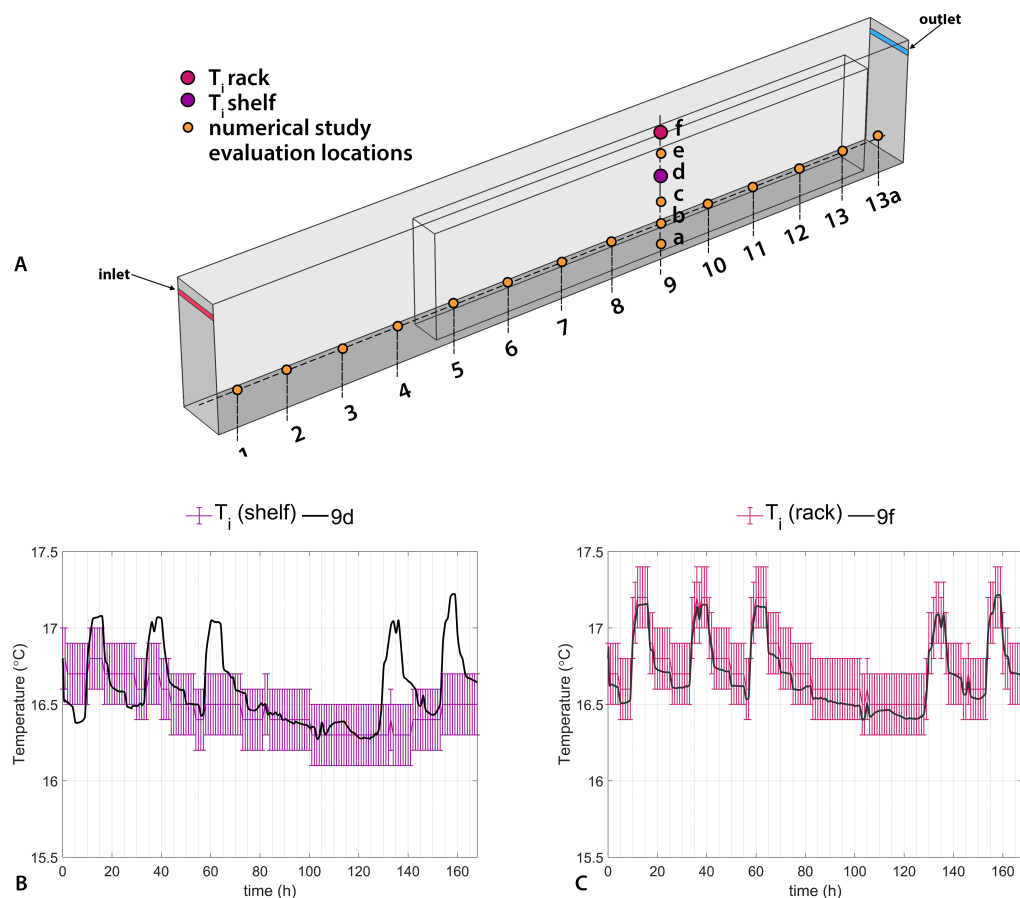


**Figure 10.** Evaluation grid locations presented in a 3D model (A). Comparison between the simulated temperature results and the measurements performed in depot 6. The measured indoor temperatures for  $T_i$  rack (pink) and  $T_i$  shelf (magenta), including equipment accuracy error bars, compared to the calculated locations 9d (B) and 9f (C).

**Table 5.** Results of the statistical operators for comparison between the measurements data and the 3D simulation results based on the configuration scenario A. The criteria range for MBE and CV RMSE is based on ASHRAE guidelines [41].

	FB (-)	FAC 1.05 (-)	MBE (%)	CV RMSE (%)
Aim	0	1	0	0
Range	(−0.3, 0.3)	>0.5	<10%	<30%
Rack (9f)	0.004	1	0.40	12.7
Shelf (9d)	−0.008	1	0.79	25.2
Box 1 (9b)	−0.022	1	2.23	<b>70.8</b>

#### 4.1.1. Indoor Climate Behavior

The results in Figure 11A show a typical colder night based on the coldest values modeled in evaluation point 9b (see Figure 10B). The external air temperature dropped below  $0^{\circ}\text{C}$  during that night. Figure 11B also shows the results of an average spring day during which the highest external air temperature during the measurement campaign was approximately  $17^{\circ}\text{C}$ , which was used during the calculations as the boundary condition on the external wall. This simulation was performed to understand the cooling effect in the archival box that was discovered during the measurements. Figure 11 shows that, as expected, a large difference between the outdoor and indoor air temperatures caused vertical temperature stratification. The air distribution mixing was not efficient due to the blockage by the archival racks. The maximum temperature difference throughout the zone was approximately  $4^{\circ}\text{C}$  (Figure 11A). When external air temperature and internal supply

air temperatures were similar to each other, this resulted in a much more homogeneous temperature distribution (Figure 11B). Temperature differences were within 0.5 °C.

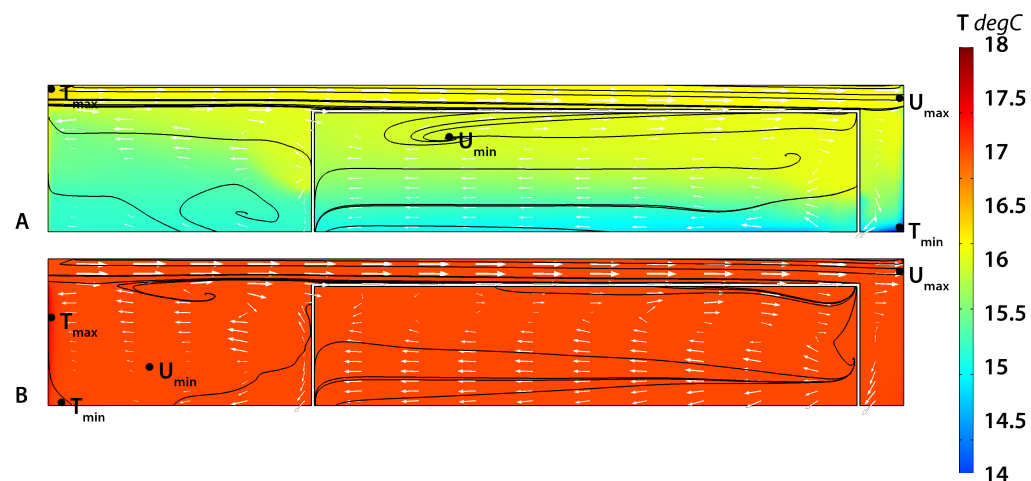


**Figure 11.** Temperature distribution and velocity streamlines inside the repository evaluated in the plane of analysis of scenario A for a cold night (14 April 2019, **A**) and a regular spring day (16 April 2019, **B**):  $T_{max,A}$  is 16.8 °C,  $T_{min,A}$  is 12.5 °C,  $U_{max,A}$  is 1.0 m/s.  $T_{max,B}$  is 17.8 °C,  $T_{min,B}$  is 17.2 °C,  $U_{max,B}$  is 1.0 m/s.  $U_{min} < 0.0001$  m/s and represents stagnant air in both cases.

#### 4.2. Scenario Study Results

In the following section, the results of the different scenarios are discussed. An overview of the scenarios can be found in Table 2. Figure 12 provides insight into the transient behavior of temperature in different evaluation points for all scenarios. The evaluation point locations are provided in the vertical cross section A–A' of Figure 12.

Appendix Figures A3 and A4 show the temperature and velocity distribution on 14 April 2019 at 04:00 h. During this time, the most extreme boundary conditions on the external wall were applied. These figures will, in addition to Figure 12, be discussed per investigated scenario in the following subsections.

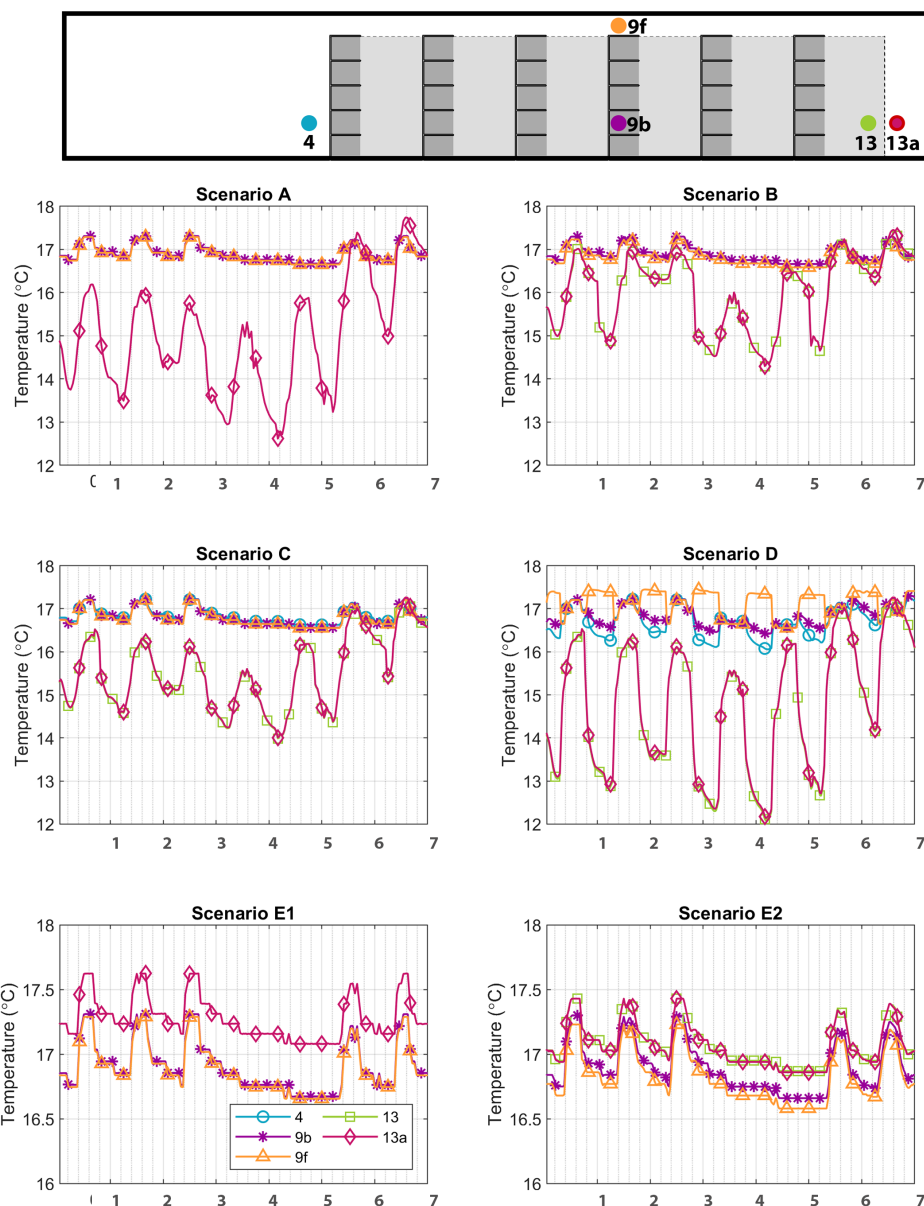


**Figure 12.** Results for the temperature evaluation in different evaluation points for the investigated scenarios. Vertical section A–A' shows the locations of the different evaluation points. Green and red (13 and 13a) are located near the external wall. Magenta (9b) is located on the center shelf, orange (9f) is located as an ambient condition position on top of a rack and blue (4) is located in front of the racks. Scenario A positioned the racks parallel to the inlet direction. Scenario B positioned the rack perpendicular to the inlet direction and Scenario C has perpendicular positioned open shelves. Scenarios E1 and E2 have a low extract compared to scenarios A–D. Scenario D has no AHU influence during closing hours.

#### 4.2.1. Archival Rack Orientation; Scenario A–C

In Figure 12, scenarios A, B and C describe the rack orientation configurations where racks oriented in parallel (A), perpendicular (B) and perpendicular with open shelves (C) to the air supply are investigated. The temperature values found in the evaluation points 13 and 13a for scenarios A–C were influenced by the external wall temperature reaching minimum temperatures during the night. A day–night cycle for  $T$  of about  $2\text{ }^{\circ}\text{C}$  was established, which is similar to the daily fluctuations found in  $T$  during the measurements

(Figure 6C). The remaining evaluation points were similar in temperature values which might indicate the sufficient distribution of air supply (see Figure 12 scenarios A–C).

Figure 11 shows that the spatial temperature distribution in between the parallel racks is fairly homogeneous. Comparing the different rack orientations (parallel, perpendicular and perpendicular with open shelves) in Figure A4 in Appendix A showed a temperature difference of 0.8 °C in between the archival racks of scenarios B and C. Both the parallel and the perpendicular rack orientations formed an obstacle and interrupted the forced airflow. This occurred especially behind the last rack near the outlet which was also observed during the measurements regarding archival box 3 (Figure 7C).

Near the external wall, lower temperatures were present in all three scenarios. In between the perpendicular placed racks, stagnant air pockets were present (Figure A4B,C in Appendix A). Modeling with open shelves provided better temperature distribution in between the racks. In most repositories, however, the shelves were filled with archival boxes which would be more accurately represented by scenario B. Scenario C provides insight for repositories with lower filling ratio's and open areas near collection (as was the case with the measurements as shown in Figure 2).

#### 4.2.2. Night Reduction; Scenario D

Scenario D uses night reduction to reduce ventilation and therefore reduce energy consumption. This scenario had the lowest wall temperature of 12.5 °C during the night. A fluctuation towards the setpoint of 16.5 °C was visible during the day considering the high fluctuation peaks in Figure 12. It took approximately 12 h to reach the setpoint at these locations before night reduction set in again. Location 9f showed interesting behavior. Increasing temperatures throughout the night due to heat transmission through the internal wall were noticeable.

In Appendix A, the temperature distribution plots with both AHU on and off are shown in Figure A3D<sub>off</sub>,D<sub>on</sub>. During night time, the negative influence of the low thermal resistance of the external wall was visible with a near wall temperature of 12.5 °C. With low temperature, a higher relative humidity will be expected near the wall surface. A gradual spreading horizontal temperature stratification was noticed in between the racks. During daytime, when the AHU is operational, a homogeneous temperature distribution was calculated.

#### 4.2.3. Air Supply and Extraction Placement; Scenario E1–E2

In terms of stable indoor climate conditions, scenarios E1 and E2 provide the least air temperature fluctuations in this study (considering the difference in x axis of Figure 12). Placing the outlet grid near the floor provided improved mixing behind the archival racks and resulted in a more homogeneous temperature distribution. Scenario E is recommended to increase the air mixing for both rack configurations.

## 5. Discussion

While legislation provides normative indoor climate requirements, meeting these proves difficult. The influence of the building envelope design and building system design on indoor climate parameters is significant. It is recommended that collection placed near external walls is monitored closely. This is mainly the case when low thermal quality walls are present in the building. While Dutch archival legislation mentions to be careful of placing objects near the floor and ceiling, no mention of adjacent areas with different climate conditions was mentioned [12]. A solution to overcome this would be to increase the thermal insulation of the building envelope, for passive buildings a U-value of 0.10–0.15 W/m<sup>2</sup>K is recommended. Increasing thermal insulation would create a buffer between external climate and indoor climate in which a low *T* would be maintained. Another option would be to look into the sufficient airflow distribution in the repository, however, this seems the less energy conserving option which, without innovative solutions, would result in an increase in the dependency on (climate control) systems. This research

could be of help for arranging the archival racks to optimize the airflow mixing of inlet conditions. The research provides interesting information for “closed” archive systems (i.e., rolling rack storage) where the racks are placed against each other with a limited form of airflow in between and the investigated fixed archival racks. Dutch archival legislation provides requirements per type of rack set-up and how much air-circulation needs to be present [12]. Further research could be performed to optimize the filling ratio of shelves in different rack configurations for increased buffering capacity.

Measurements and numerical modeling provide insight into the climate conditions in repositories. While it is common to monitor the ambient indoor air conditions of a space or in the HVAC return duct, the experimental part of the research shows that locally deviating indoor climates are present and the ambient indoor conditions do not represent the hygrothermal conditions of the repository inside archival boxes. While stable  $T$  and  $RH$  are required by legislation, this study shows that even though an HVAC system is present, stable conditions might not be maintained and near the external wall, daily  $T$  fluctuations occur.  $T/RH$  cycling seems not to be of influence for chemical degradation and preventing fluctuations is not necessary from a chemical decay point of view [42]. This would underscore the idea of using passive ways to maintain preservation conditions (specifically low, stable  $T$  which results in a stable  $RH$ ) in archival facilities where daily fluctuations are almost canceled out but seasonal fluctuations do gradually occur [17]. With passive or semi-passive measures, the effect on the accumulation of volatile organic compounds (VOCs) needs to be considered [23,43].

A limitation of the current study is the lack of extensive validation based on air velocity distribution measurements. The numerical study was used as a means to understand the hygrothermal measurement results. For this, the inlet velocity was measured short-term and compared with the building management system velocity. The building management system inlet velocity was used as an imposed boundary condition. To gain more accuracy in the numerical model, the calculated air distribution needs to be compared with measurements.

The microclimate measured during the experimental campaign was influenced by the thermal radiance of the external wall. Both boxes, 3 (closest to external wall) and 1 (in the center of the repository), showed influence with a dropped  $T_{\text{archivalbox}}$ . This complies with the results mentioned in studies such as those of Wilson et al., Clare et al. and Bigourdan et al. where the microclimate monitored in archival boxes showed a time delay of a few days [27–29]. Comparing both the microclimate in the archival box and just outside of the archival box, the trend shown in the two results is similar (see Figure 7). Therefore, the degradation risks for objects placed in or out of an archival box would most likely be similar when it comes to incorrect  $T$  and  $RH$ . In the correct case, there was a cooling effect which did not increase the risk of archival objects that prefers preservation specifications with a low  $T$ . Further research could account for thermal and hygric buffering of the archival box and to what extent this reduces the degradation risk during long periods of warm external temperatures.

Based on the research questions described in the introduction, the following conclusions can be drawn:

- Measurements show that the microclimate in an archival box has a small daily span for  $T$  and  $RH$ . A stable daily climate surrounds the archival collection inside the box. The seasonal span for the  $T$  and  $RH$  of the archival box near an external wall shows larger fluctuations compared to other positions in the archival rack. This is mainly due to the influence of the external wall radiation which is also experienced by objects outside archival boxes placed near the external wall. Since relative humidity does not exceed 65% for a long period to form biological risk issues and short-term (hourly) fluctuations in temperature do not exceed 1 °C, preservation conditions are considered good inside the archive box even when the conditions do not meet the criteria set by the Dutch archival legislation.  $T$  is on average lower than legislation prescribes. During summer, this significantly increases cooling energy consumption .

- The simulated scenarios with archival racks perpendicular to the inlet direction show low velocities between the racks. Placing the racks in a parallel orientation ensures air-movement and therefore air-mixing between the racks. Fixed archival racks with a low fill rate create local indoor microclimates in between objects or shelves. Completely filled archival racks have the convenience of high thermal and hygric buffering by the objects, while short-term fluctuations will have a limited effect on the core of the objects due to this buffering capacity.
- According to the numerical model, scenario D (night reduction in which the AHU is turned off) provides the largest temperature fluctuation near the external wall with  $4^{\circ}\text{C}$ . The fluctuation occurs gradually over a time period of 12 h ( $\approx 0.35^{\circ}\text{C}/\text{h}$ ). Turning off the AHU in a repository indicates the greater influence of indoor temperature towards the building envelope quality. In the case of a low thermal quality, this results in temporal gradients near the external walls. If the thermal quality of an external wall is good, very limited influence of the external climate is expected and energy conservation increases. A small amount of ventilation might be needed to remove the volatile organic compounds emitted by objects or building materials.
- The duct placement of an HVAC system assists in creating vertical stratification when both the supply and extract are located near the ceiling. This results in limited airflow. Low external wall quality contributes to a horizontal stratification when air-mixing is blocked by objects such as archival racks. Improving airflow for better air-mixing near an external wall is achieved by placing the outlet grid near the floor next to the external wall.

**Author Contributions:** Contributions made by the authors were as follows: conceptualization: K.K., methodology: K.K. and H.L.S.; validation: K.K.; data analysis: K.K., B.A. and H.L.S.; writing: K.K.; review and editing: K.K., R.P.K., B.A. and H.L.S.; supervision: R.P.K., B.A. and H.L.S.; project administration: H.L.S. All authors have read and agreed to the published version of the manuscript.

**Funding:** This research received no external funding.

**Institutional Review Board Statement:** Not applicable.

**Informed Consent Statement:** Not applicable.

**Data Availability Statement:** Experimental data is stored at (<http://www.monumenten.bwk.tue.nl/>) accessed on 31 March 2021). This data is available for the authors and case study.

**Acknowledgments:** The authors would like to express their gratitude to the archive case study for participating and cooperating in this study. A special thanks goes out to Cor de Graaf, Edith Greuter and Henk Heijmans for their expertise and willingness to help with the experimental campaign.

**Conflicts of Interest:** The authors declare no conflicts of interest.

## Appendix A

Figure A1 shows the building plan of the investigated building. Figure 3 in the main text shows the building from the perspective of the public entrance. The repository tower (orange) was an addition to the back of the building comprised of 5 stories.



**Figure A1.** Building plan of the investigated buildings ground floor.

In order to have a global insight into the hygrothermal indoor climate, Table A1 provides multiple statistical properties of the used measurement data.

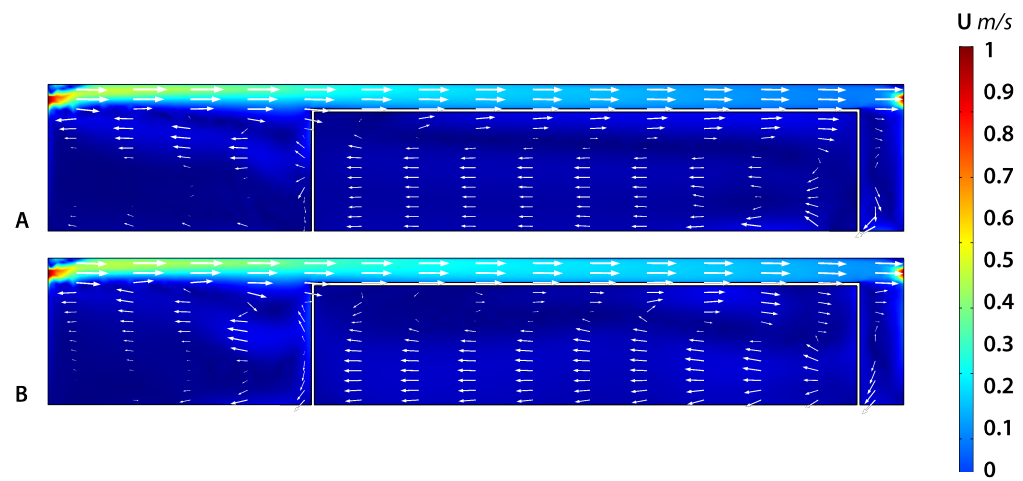
Though air velocity was not extensively validated with measurements, the CFD model provides an indication of the occurring flow field. Limited air mixing was present near the external wall, as can be seen in Figure A2. Stagnant air might increase the risk of mold growth in combination with  $T$  and  $RH$  conditions favorable for mold germination. Improving air-mixing by ventilation is mainly sought to prevent internally generated pollutants that could harm susceptible objects [17,23].

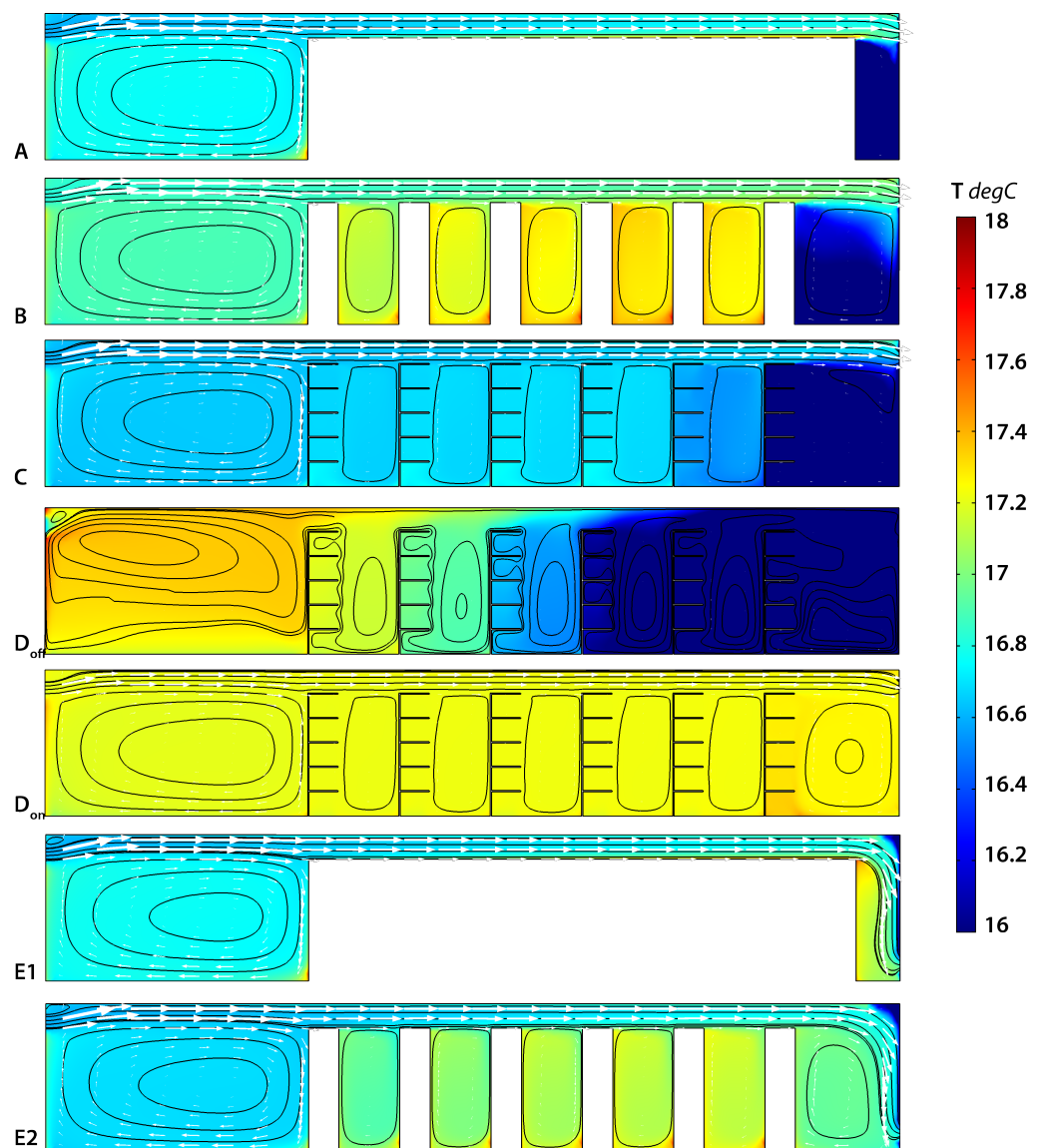
Figure A3 shows the numerical results of all scenarios. With the exception of Figure A3  $D_{on}$ , all temperature distribution plots were calculated for 14 April at 04:00 h. During the night, the temperature stratification was the largest, especially for scenario  $D_{off}$ . Table A2 shows the minimum and maximum temperatures and velocities. A horizontal temperature gradient of 0.57K/m was present for scenario  $D_{off}$  while air speed was 0 m/s (Figure A4  $D_{off}$ ).

Figure A4 provides the results of velocity calculations per scenario. Overall, the same airflow distribution is present. The influence of the position of the archival racks had limited influence on the airflow. Increased velocity and circulation are visible near the external wall when the extract of the AHU is placed lower.

**Table A1.** Results for ambient and surface conditions during the year 2018: statistical properties.

	$T_{y,av}$ (°C)	$T_{y,av,min}$ (°C)	$T_{y,av,max}$ (°C)	$\Delta T$ (K/h)	$\Delta T_{std}$ (K/h)	$\Delta T$ (K/d)	$\Delta T_{std}$ (K/d)	$\Delta T$ (K/w)	$\Delta T_{std}$ (K/w)	$RH_{y,av}$ (%)	$RH_{y,av,min}$ (%)	$RH_{y,av,max}$ (%)	$\Delta RH$ (%/h)	$\Delta RH_{std}$ (%/h)	$\Delta RH$ (%/d)	$\Delta RH_{std}$ (%/d)	$\Delta RH$ (%/w)	$\Delta RH_{std}$ (%/w)
Depot 3	17.1	-0.2	0.2	0.1	0.1	0.5	0.4	1.0	0.3	57.1	-2.6	1.6	0.5	0.6	2.4	1.2	4.8	1.7
depot 4	16.0	-0.1	0.2	0.1	0.1	0.4	0.2	0.8	0.2	56.5	-2.2	1.6	0.5	0.6	2.1	1.0	4.1	1.5
Depot 5	16.6	-0.5	0.7	0.1	0.1	0.3	0.2	0.8	0.3	58.0	-1.9	1.8	0.5	0.5	1.9	0.9	4.1	1.7
Depot 6	16.7	-0.4	0.6	0.1	0.1	0.6	0.3	1.1	0.3	57.8	-1.3	1.4	0.4	0.4	2.1	1.0	4.2	1.4
Depot 6 wall east	15.7	-1.3	1.0	0.0	0.1	0.3	0.1	0.8	0.4	59.8	-1.4	2.7	0.7	0.8	2.1	1.2	3.9	1.6
$T_{surf}$	16.1	-1.3	1.1	0.0	0.0	0.2	0.1	0.7	0.4									
Depot 6 wall west	15.8	-2.5	2.3	0.1	0.1	1.1	0.5	2.3	0.8	61.7	-6.1	7.5	0.7	0.7	3.8	1.7	7.2	2.2
$T_{surf}$	15.8	-2.8	2.5	0.1	0.1	1.0	0.5	2.4	0.9									
Depot 6 shelf	16.4	-0.7	0.6	0.0	0.0	0.1	0.1	0.5	0.2	58.6	-0.9	1.0	0.1	0.2	0.6	0.5	1.5	0.9
Depot 6 box 1	16.3	-1.3	1.1	0.0	0.0	0.2	0.1	0.7	0.4	59.2	-1.8	2.7	0.0	0.1	0.4	0.4	1.5	1.0
Depot 7	17.1	-0.3	0.4	0.1	0.1	0.4	0.2	0.8	0.3	56.6	-3.5	2.7	0.9	1.1	2.8	1.6	5.4	2.1

**Figure A2.** Time-averaged velocity distribution plot of scenario 1 with the plane of analysis in between archive racks. Outdoor  $T$  was below 0 °C on 14 April 2019 at 04:00 h (A). (B) shows the results for 16 April when the external  $T$  was 17 °C at 14:00 h. The white arrows represent the proportional velocity in a calculation grid.



**Figure A3.** Time-averaged temperature distribution plot of all modeled scenarios (A–E2) when outdoor  $T$  was below  $0\text{ }^{\circ}\text{C}$  on 14 April 2019 at 04:00 h. The figures are time-averaged over 30 min of calculations. The figure for scenario  $D_{on}$  shows the results for 16 April when the external  $T$  was  $17\text{ }^{\circ}\text{C}$  at 14:00 h. The velocity streamlines are shown in black and the white arrows represent the proportional velocity in a calculation grid.

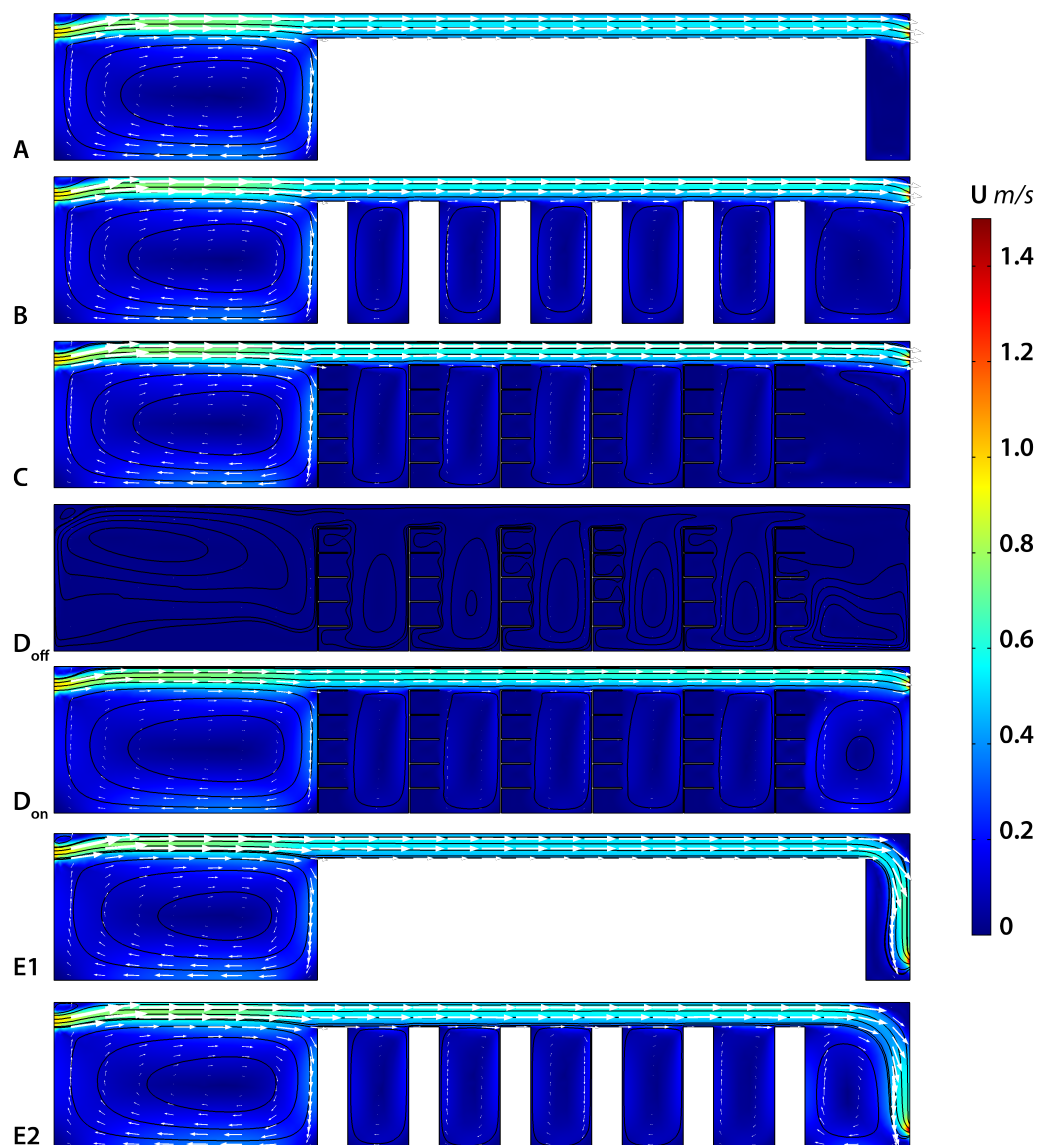


**Figure A4.** Time-averaged velocity distribution plot of all modeled scenarios (A–E2) when the outdoor  $T$  was below  $0\text{ }^{\circ}\text{C}$  on 14 April 2019 at 04:00 h. The figures are time-averaged over 30 min of calculations. The figure for scenario  $D_{on}$  shows the velocity results for 16 April when the external  $T$  was  $17\text{ }^{\circ}\text{C}$  at 14:00 h. The velocity streamlines are shown in black and the white arrows represent the proportional velocity in a calculation grid.

**Table A2.** Minimum and maximum values for the temperature and velocity found for all modeled scenarios when the outdoor  $T$  was below  $0\text{ }^{\circ}\text{C}$  on 14 April 2019. The values found for scenario  $D_{on}$  show the results for 16 April when the external  $T$  was  $17\text{ }^{\circ}\text{C}$ .

	A	B	C	$D_{off}$	$D_{on}$	E1	E2
$T_{min}$ ( $^{\circ}\text{C}$ )	10.4	14.4	11.6	9.9	16.9	14.7	13.2
$T_{max}$ ( $^{\circ}\text{C}$ )	17.8	17.8	17.2	18.0	17.6	17.9	17.7
$U_{min}$ (m/s)	$2.6 \times 10^{-5}$	$4.2 \times 10^{-5}$	$4.8 \times 10^{-6}$	0	0	$3.8 \times 10^{-5}$	$2.9 \times 10^{-5}$
$U_{max}$ (m/s)	1.4	1.5	1.5	0.16	1.5	1.6	1.6

## References

1. Curteis, T. The Cathedrals of England: Environmental Performance, Conservation and Exhibitions. *Stud. Conserv.* **2018**, *63*, 70–75. [[CrossRef](#)]
2. Janssen, H.; Christensen, J.E. Hygrothermal optimisation of museum storage spaces. *Energy Build.* **2013**, *56*, 169–178. [[CrossRef](#)]
3. Thomson, G. *The Museum Environment*; Butterworths-Heinemann: London, UK, 1978.
4. Camuffo, D. *Microclimate for Cultural Heritage*; Elsevier B.V.: Amsterdam, The Netherlands, 2014.
5. Lucchi, E. Review of preventive conservation in museum buildings. *J. Cult. Herit.* **2018**, *29*, 180–193. [[CrossRef](#)]
6. Linden, J.; Reilly, J.; Herzog, P. Research on energy savings opportunities in university libraries. *Libr. Hi Tech* **2012**, *30*, 384–396. [[CrossRef](#)]
7. Brimblecombe, P. The balance of environmental factors attacking artifacts. In *Durability and Change—The Science, Responsibility and Cost of Sustaining Cultural Heritage*; Krumbein, W., Brimblecombe, P., Cosgrove, D., Staniforth, S., Eds.; Wiley: London, UK, 1994; pp. 67–79.
8. Bonora, A.; Fabbri, K. Two new indices for preventive conservation of the cultural heritage: Predicted risk of damage and heritage microclimate risk. *J. Cult. Herit.* **2020**, *47*, 208–217.
9. Lucchi, E. Environmental Risk Management for Museums in Historic Buildings through an Innovative Approach: A Case Study of the Pinacoteca di Brera in Milan (Italy). *Sustainability* **2020**, *12*, 5155. [[CrossRef](#)]
10. British Standards Institute. *BS 5454 Recommendations for the Storage and Exhibition of Archival Documents*; British Standards Institute: London, UK, 2000.
11. British Standards Institute. *PD 5454:2012 Publication Guide for the Storage and Exhibition of Archival*; British Standards Institute: London, UK, 2012.
12. Ministerie van Onderwijs Cultuur en Wetenschap. *Dutch Archival Legislation—Archiefwet*; Ministerie van Onderwijs Cultuur en Wetenschap: Den Haag, The Netheralnds, 1995.
13. Kramer, R.; van Schijndel, J.; Schellen, H. Dynamic setpoint control for museum indoor climate conditioning integrating collection and comfort requirements: Development and energy impact for Europe. *Build. Environ.* **2017**, *118*, 14–31. [[CrossRef](#)]
14. Kompatscher, K.; Kramer, R.; Ankersmit, B.; Schellen, H. Intermittent conditioning of library archives: Microclimate analysis and energy impact. *Build. Environ.* **2019**, *147*, 50–66. [[CrossRef](#)]
15. Hong, S.H.; Strlič, M.; Ridley, I.; Ntanios, K.; Bell, N.; Cassar, M. Climate change mitigation strategies for mechanically controlled repositories: The case of The National Archives, Kew. *Atmos. Environ.* **2012**, *49*, 163–170. [[CrossRef](#)]
16. Steeman, M.; De Paepe, M.; Janssens, A. Impact of whole-building hygrothermal modelling on the assessment of indoor climate in a library building. *Build. Environ.* **2010**, *45*, 1641–1652. [[CrossRef](#)]
17. Padfield, T.; Larsen, P.K.; Jensen, L.A.; Ryhl-svendsen, M.; Reyden, D.E.R. The potential and limits for passive air conditioning of museums, stores and archives. In *Museum Microclimates*; National Museum of Denmark: Lyngby, Denmark, 2007; pp. 191–197.
18. Knudsen, L.R. Performance of Danish Low-Energy Museum Storage Buildings. In Proceedings of the ICOM-CC18th Triennial Meeting, Copenhagen, Denmark, 4–8 September 2017.
19. Padfield, T.; Ryhl-Svendsen, M.; Larsen, P.K.; Aasbjerg Jensen, L. A Review of the Physics and the Building Science which Underpins Methods of Low Energy Storage of Museum and Archive Collections\*. *Stud. Conserv.* **2018**, *63*, 209–215. [[CrossRef](#)]
20. Ryhl-Svendsen, M.; Jensen, L.A.; Larsen, P.K.; Bøhm, B.; Padfield, T. Ultra-low-energy museum storage. In Proceedings of the ICOM-CC 16th Triennial Conference, Lisbon, Portugal, 19–23 September 2011.
21. Bohm, B.; Ryhl-Svendsen, M. Analysis of the thermal conditions in an unheated museum store in a temperate climate. on the thermal interaction of earth and store. *Energy Build.* **2011**, *43*, 3337–3342. [[CrossRef](#)]
22. Diulio, M.d.I.P.; Mercader-Moyano, P.; Gómez, A.F. The influence of the envelope in the preventive conservation of books and paper records. Case study: Libraries and archives in La Plata, Argentina. *Energy Build.* **2019**, *183*, 727–738. [[CrossRef](#)]
23. Smedemark, S.H.; Ryhl-Svendsen, M.; Toftum, J. Distribution of temperature, moisture and organic acids in storage facilities with heritage collections. *Build. Environ.* **2020**, *175*, 106782. [[CrossRef](#)]
24. Holl, K.; Kilian, R.; Klemm, L.; Lengsfeld, K.; Bichlmair, S.; Krus, M. Sustainable Museum Storage Buildings for Long-term Preservation. *Stud. Conserv.* **2018**, *63*, 366–368. [[CrossRef](#)]
25. Krus, M.; Rösler, D.; Klemm, L. Hygrothermal Simulations of Energy-saving Measures to Stabilize the Internal Environment of an Archive Depot. In Proceedings of the Clima 2013—11th REHVA World Congress and 8th International Conference on IAQVEC “Energy Efficient, Smart and Healthy Buildings”, Prague, Czech Republic, 16–19 June 2013.
26. Pavlogiorgatos, G. Environmental parameters in museums. *Build. Environ.* **2003**, *38*, 1457–1462. [[CrossRef](#)]
27. Wilson, H.; Vansnick, S. The effectiveness of dust mitigation and cleaning strategies at The National Archives, UK. *J. Cult. Herit.* **2017**, *24*, 100–107. [[CrossRef](#)]
28. Clare, H.; Farmer, R.; Ntanios, K. The Study of Microclimates within Storage Boxes of Archival Records. 2014. Available online: [https://www.culturalheritage.org/docs/default-source/annualmeeting/2014am\\_poster58\\_investigation\\_into\\_microclimates.pdf?sfvrsn=2](https://www.culturalheritage.org/docs/default-source/annualmeeting/2014am_poster58_investigation_into_microclimates.pdf?sfvrsn=2) (accessed on 18 May 2019).
29. Bigourdan, J.L. *Methodologies for Sustainable HVAC Operation in Collection Environments*; Image Permanence Institute: Rochester, NY, USA, 2017. [[CrossRef](#)]
30. Ferreira, C.; de Freitas, V.P.; Delgado, J.M. The Influence of Hygroscopic Materials on the Fluctuation of Relative Humidity in Museums Located in Historical Buildings. *Stud. Conserv.* **2020**, *65*, 127–141. [[CrossRef](#)]

31. Sensors; Eltek: Cambridge, UK, 2016.
32. Adan, O.C.G. On the Fungal Defacement of Interior Finishes. Ph.D. Thesis, Eindhoven University of Technology, Eindhoven, The Netherlands, 1994.
33. Michalski, S. Double the life for each five-degree drop, more than double the life for each halving of relative humidity. In Proceedings of the Thirteenth Triennial Meeting ICOM-CC, Rio de Janeiro, Brazil, 22–27 September 2002; Number 3, pp. 66–72.
34. COMSOL AB. COMSOL Multiphysics® v.5.2a; COMSOL AB: Stockholm, Sweden, 2016.
35. Steeman, H.J. Modelling Local Hygrothermal Interaction between Airflow and Porous Materials for Building Applications. Ph.D. Thesis, Ghent University, Gent, Belgium, 2009.
36. Coakley, D.; Raftery, P.; Keane, M. A review of methods to match building energy simulation models to measured data. *Renew. Sustain. Energy Rev.* **2014**, *37*, 123–141. [[CrossRef](#)]
37. Kramer, R.; van Schijndel, J.; Schellen, H. Inverse modeling of simplified hygrothermal building models to predict and characterize indoor climates. *Build. Environ.* **2013**, *68*, 87–99. [[CrossRef](#)]
38. Coelho, G.B.; Silva, H.E.; Henriques, F.M. Calibrated hygrothermal simulation models for historical buildings. *Build. Environ.* **2018**, *142*, 439–450. [[CrossRef](#)]
39. Schatzmann, M.; Olesen, H.; Franke, J. Cost 732 Model Evaluation Case Studies: Approach and Results; Number 732; COST Office: Brussels, Belgium, 2010; p. 732.
40. Sedlbauer, K. Prediction of Mould Fungus Formation on the Surface of/and Inside Building Components; Fraunhofer Institute for Building Physics: Stuttgart, Germany, 2001; p. 247.
41. ASHRAE. ASHRAE Guideline 14—Measurement of Energy, Demand and Water Savings; Technical report; ASHRAE: Atlanta, GA, USA, 2014.
42. Bigourdan, J.L.; Reilly, J.M. Effects of Fluctuating Environments on Paper Materials - Stability and Practical Significance for Preservation. In Proceedings of the La Conservation à l’Ère du Numérique, Actes des Quatrièmes Journées Internationales d’Études de l’ARSAG, Paris, France, 27–30 May 2002; pp. 1–37.
43. Pasquarella, C.; Balocco, C.; Saccani, E.; Capobianco, E.; Viani, I.; Veronesi, L.; Pavani, F.; Pasquariello, G.; Rotolo, V.; Palla, F.; et al. Biological and microclimatic monitoring for conservation of cultural heritage: A case study at the De Rossi room of the Palatina library in Parma. *Aerobiologia* **2020**, *36*, 105–111. [[CrossRef](#)]